

UCRL- 93332  
PREPRINT

**CIRCULATION COPY**  
SUBJECT TO RECALL  
IN TWO WEEKS

THE ELECTRONIC THERMODYNAMICS OF IRON  
UNDER EARTH CORE CONDITIONS

A. K. McMahan  
Lawrence Livermore National Laboratory  
University of California  
Livermore, CA 94550

This paper was prepared for submittal to  
Physics of the Earth Planetary Interiors

September 1985

Lawrence  
Livermore  
National  
Laboratory

This is a preprint of a paper intended for publication in a journal or proceedings. Since changes may be made before publication, this preprint is made available with the understanding that it will not be cited or reproduced without the permission of the author.

#### DISCLAIMER

This document was prepared as an account of work sponsored by an agency of the United States Government. Neither the United States Government nor the University of California nor any of their employees, makes any warranty, express or implied, or assumes any legal liability or responsibility for the accuracy, completeness, or usefulness of any information, apparatus, product, or process disclosed, or represents that its use would not infringe privately owned rights. Reference herein to any specific commercial products, process, or service by trade name, trademark, manufacturer, or otherwise, does not necessarily constitute or imply its endorsement, recommendation, or favoring by the United States Government or the University of California. The views and opinions of authors expressed herein do not necessarily state or reflect those of the United States Government or the University of California, and shall not be used for advertising or product endorsement purposes.

## Abstract

The LMTO method is used to calculate the electronic band structure of iron in the  $\epsilon$ -phase (hcp) and in the  $\gamma$ -phase (fcc) for seven compressions from 4 to 980 GPa. The electronic specific heat  $c_v(T)$  is calculated for each phase by numerical integration from the resultant density of states. Previous work is thus supported for  $\gamma$ -iron and extended to  $\epsilon$ -iron, the most likely inner core component. A simple parameterization of  $c_v$  is given for use in making geophysical estimates. Other thermodynamic parameters which are calculated are the electronic free energy, the thermal electronic pressure, and an electronic Gruneisen parameter,  $\gamma_e$ .

Recent studies of liquid iron and iron alloys indicate that the density of states at the Fermi level does not differ much from that calculated for pure crystalline iron. We cautiously apply our results to the outer core and find that  $c_v = 1.8 \pm 0.5R$  and  $\gamma_e = 1.3 \pm 0.4$ . This indicates that the total heat capacity of the core is one-quarter that of the entire Earth.



## 1. Introduction

Constraints on our geophysical understanding of the deep earth can be provided by experimental and theoretical study of the high-pressure, high-temperature physics of iron, which is thought to be a major core component. Brown and McQueen (1982) pointed out that shock wave experimental data can provide tighter constraints if we better knew the important auxiliary parameters, the heat capacity and the Gruneisen parameter. Since these parameters are currently not well constrained by experiment we must turn to the available theory of transition metal physics.

We report here a theoretical study of the electronic thermodynamics, under large compressions, for two phases of iron, the  $\epsilon$ -phase (hcp structure), thought to constitute the inner core (Brown and McQueen, 1982), and the  $\gamma$ -phase (fcc structure). Such electronic effects are significant under core conditions -- we calculate for iron a heat capacity more than 50% larger than that given by the classical Dulong and Petit value of  $3R$ , where  $R$  is the gas constant.

Previous work involving electronic band structure calculation for iron has concentrated almost exclusively on the low pressure - low temperature phase,  $\alpha$ -iron (bcc structure). Callaway and Wang (1977) applied the linear combination of Gaussian orbitals (LCGO) method in a self-consistent, spin polarized calculation for ferromagnetic iron. They found the best agreement with experimental data for the exchange and correlation potential of von Barth and Hedin (1972). Moruzzi *et al.* (1978) performed a Kohn-Korringa-Rostoker (KKR) calculation on  $\alpha$ -iron with the muffin-tin approximation to the potential (Janak, 1974).

Pressure has seldom been incorporated into iron band structure work. Recently Vinturova *et al.* (1979) used a model KKR Hamiltonian to calculate compressional effects on ferromagnetic iron. Johnson *et al.* (1984) applied the APW method to calculate spin-polarized energy bands at the normal lattice constant and at lattice spacings corresponding to approximate pressures of 128 and 256 kbar. A phase transition from

$\alpha$ -iron to  $\epsilon$ -iron occurs at 130 kbar (Jamieson and Lawson, 1962); however, the 256 kbar calculation of Johnson *et al.* (1984) was performed in order to check for a linear variation of the extremal areas of the Fermi surface with pressure.

Bukowinski (1976,1977) calculated the band structure for  $\gamma$ -iron to obtain an equation of state under inner core conditions. The muffin-tin form of the potential was used and the energy eigenvalues were calculated at 19 points in the reduced Brillouin zone for this APW calculation. A major result of his work is the elimination of electronic transition as a viable explanation for the existence of the inner core - outer core discontinuity. His work indicated that the electronic structure of  $\gamma$ -iron is stable to at least two-fold compression. However, the pressure given by the equation of state is too large for a given volume.

The other close-packed form of iron was considered by Young and Grover (1984), who constructed a semiempirical equation of state for  $\epsilon$ -iron. By dividing the total energy into mean field, interatomic pair potential, and electronic thermal terms, they used five adjustable parameters for fits to the available data defining the experimental isotherm, Hugoniot, and melting curve. The equation of state thus obtained is the basis for the pressure calibration used in the present work.

We calculate the electronic band structure of both  $\epsilon$ -iron and  $\gamma$ -iron using the accurate, yet computationally efficient, linear muffin-tin orbital method (LMTO), described at length elsewhere (Andersen, 1975, 1983; Andersen and Jepsen, 1977; Skriver, 1984). Jepsen *et al.* (1975) used the LMTO method to calculate the band structure for the hcp metals zirconium, hafnium, ruthenium, and osmium. Although they did not consider the effect of compression, it is encouraging that the several band structures they computed with this method yield Fermi surfaces that are in excellent agreement with available de Haas-van Alphen measurements, indicating that the calculated d-band position is typically misplaced by less than 10 mRy ( $\approx 2 \times 10^{-20}$  J).

Since neither  $\epsilon$ -iron nor  $\gamma$ -iron is expected to display magnetic order at core

temperatures, it is not necessary to include spin coupling effects in band structure calculations for these two phases. Mossbauer measurements down to 0.030 K detected no measureable hyperfine field for  $\epsilon$ -iron in the pressure range from 1 bar to 215 kbar (Cort *et al.*, 1982; Williamson *et al.*, 1972). Neutron scattering measurements at 1320 K revealed  $\gamma$ -iron to be paramagnetic with a moment of  $0.9 \pm 0.1 \mu_B$  (Brown *et al.*, 1983). A close-packed liquid iron alloy at much higher temperatures is more unlikely yet to possess magnetic order, even under an applied magnetic field such as is generated in the outer core.

High-temperature thermodynamics based on the electronic energy distribution are computed in the present work using Fermi-Dirac statistics to thermally populate accessible single electron states. This quantum-statistical approach is the correct formalism to treat thermodynamic properties associated with conduction electrons.

We emphasize that the current band structure calculations are for pure solid iron. The inner core of the earth is almost certainly solid, as is evidenced by observations of spheroidal shear modes (Masters and Gilbert, 1981) and of body wave phases (Choy and Cormier, 1983). It is believed that such solidity results from the freezing of pure iron out of an outer core mixture of iron and one or more lighter alloying elements. However, the outer core is about twenty times as massive as the inner core, and hence any band structure calculation that successfully treats the electronic properties of a liquid iron alloy under high pressure and temperature is of geophysical interest. Unfortunately, it is difficult to theoretically model the electronic properties of liquids and alloys. The additional complexities imposed by transition metal orbital structure and the geophysical requirement of extreme conditions make complete theoretical treatment of candidate outer core mixtures an elusive goal at the present time. We discuss this point in section 5.

## 2. Electronic Density of States

The electronic densities of states for the two phases of iron were obtained using the LMTO method as presented in Skriver (1984). The combined-correction term to the LMTO method was included, the exchange-correlation potential of von Barth and Hedin (1972) was assumed, and angular momentum components through  $f$  character were retained.

Our calculation used no adjustable parameters, such as  $\alpha$ , the exchange parameter of Slater's  $X-\alpha$  method for approximating the effect of exchange and correlation (Slater, 1974). Bukowinski (1976) determined  $\alpha$  in his calculation by demanding that the pressure, as calculated from the virial theorem, be zero at the experimentally estimated 0 K lattice constant of  $\gamma$ -iron. The LMTO method implicitly uses an  $\alpha = 2/3$  for the exchange-only part of the potential (Skriver, 1984).

All reported results here are from nonrelativistic calculations. Test scalar relativistic calculations, in which all relativistic contributions except spin orbit are included, were carried out at one compression and resulted in slight changes in the density of states and only a 1% change in the electronic specific heat.

The valence band structure was computed on meshes of 150 and 240 points per irreducible wedge for the hcp and fcc structures, respectively, after obtaining one-electron potentials from calculations in which all electrons are treated self-consistently. The tetrahedral method (Skriver, 1984) was then used to obtain the electronic density of states on an energy grid having approximately 134 points between the bottom of the  $4s$  band and the Fermi level. Test hcp calculations using 252 points per irreducible wedge had negligible effect on the calculated electronic specific heat, while more than doubling the energy grid over which the density of states was calculated changed the calculated specific heat by only 1%.

Calculations were carried out for each structure at six compressions  $V/V_0$ , corresponding to values of the Wigner-Seitz radius  $R_{WS} = 2.6, 2.5, \dots, 2.0$  bohr, where

$V = \frac{4}{3}\pi R_{WS}^3$  is the volume per atom in the solid. These cellular parameters correspond to pressures of near zero to more than five megabars. We further discuss pressure calibration in section 4.

Plots of the density of states for four intermediate compressions are shown in Fig. 1 for  $\gamma$ -iron and in Fig. 2 for  $\epsilon$ -iron. A vertical line indicates the Fermi energy for each plot. Clearly evident in these figures are large fluctuations in the density of states for the 3d bands superimposed on the relatively low background of comparatively free-electron-like 4s and 4p electrons. The sharp structure especially noticeable in the 3d part of the density of states includes non-differentiable points, the van Hove singularities (see, e.g., Ashcroft and Mermin, 1976). Superposition of the density of states plots for both close-packed phases at any given compression reveals close correspondence in shape, implying that calculated electronic physical properties should be similar for the two phases. A density of states plot for non-close-packed  $\alpha$ -iron is different in overall shape from that of iron in the other two structures (see, e.g., Moruzzi *et al.*, 1978).

### 3. Calculation of the Specific Heat

Typically the electronic specific heat at non-zero temperature is derived from density of states curves via the Sommerfeld expansion for integrals with the Fermi function in the integrand (Ashcroft and Mermin, 1976). Since the electronic specific heat at constant volume is given by

$$c_v = \left( \frac{\partial u_e}{\partial T} \right)_v, \quad (2)$$

we must know the total electronic energy  $u_e$  as a function of temperature. Fortunately it has been previously demonstrated (McMahan and Ross, 1977) that up to a temperature of at least 20,000 K it is possible to accurately represent the temperature-dependent part of this energy by simply summing over the *zero-temperature* one-electron eigenvalues  $E$ , or in terms of the density of states  $g(E)$ ,

$$u_e = \int_0^{\infty} dE g(E) E f(E), \quad (3)$$

where  $f(E)$  is the fermi distribution function:

$$f(E) = \frac{1}{e^{(E-\mu)/kT} + 1}. \quad (4)$$

Similar form is shown by the equation for electron number density,

$$n_e = \int_0^{\infty} dE g(E) f(E). \quad (5)$$

These integrals are of the general form  $\int_{-\infty}^{\infty} dE H(E) f(E)$ . Because of the shape of

the Fermi function  $f(E)$ ,  $\int_{-\infty}^{\infty} dE H(E) f(E)$  deviates from its zero temperature value,

$E_F$   
 $\int_{-\infty}^{\infty} dE H(E)$ , due only to the contributions from the energy range about  $\mu$  of width a

few  $kT$ . If there are no rapid variations of  $H(E)$  in this energy range then the temperature dependence of the integral should be given accurately by representing  $H(E)$  by the first few terms of its Taylor expansion about  $E = \mu$ :

$$H(E) = \sum_{n=0}^{\infty} \frac{d^n}{dE^n} H(E) \Big|_{E=\mu} \frac{(E-\mu)^n}{n!}. \quad (6)$$

This leads to the explicit form of the Sommerfeld expansion:

$$\int_{-\infty}^{\infty} dE H(E) f(E) = \int_{-\infty}^{\mu} dE H(E) + \frac{\pi^2}{6} (kT)^2 H'(\mu) + \frac{7\pi^4}{360} (kT)^4 H'''(\mu) + O\left\{\frac{kT}{\mu}\right\}^6. \quad (7)$$

Successive terms in this expansion become relatively smaller by  $O(kT/\mu)^2$  which is  $O(10^{-4})$  at room temperature for a free electron gas.

If the expansion is truncated beyond terms of order  $T^2$  then the chemical potential is given by

$$\mu = E_F - \frac{\pi^2}{6} (kT)^2 \frac{g'(E_F)}{g(E_F)}. \quad (8)$$

The electronic energy density at constant number density becomes

$$u_e = u_{e,0} + \frac{\pi^2}{6} (kT)^2 g(E_F), \quad (9)$$

yielding the electronic specific heat at constant volume:

$$c_v = \frac{\pi^2}{3} k^2 T g(E_F). \quad (10)$$

The accuracy of the approximation given by Eq. (10) is only as good as the assumptions inherent in the Sommerfeld expansion. For iron at temperatures and pressures achievable in shock wave experiments the successive terms in the expansion drop off one hundred times as slowly as for a free electron gas at room temperature. (Increasing pressure acts to increase  $\mu$  and hence further diminish successive terms in the expansion, but the elevated temperature more than compensates for this effect.) This makes each term about 1% as large as the one before it, so few terms (and hence few orders of derivatives of  $H(E)$ ) still are necessary to accurately represent the expansion.

A more important reason to question use of the Sommerfeld expansion in the derivation of an expression for the electronic specific heat of iron arises upon examination of the complex structure of the density of states  $g(E)$ . As noted above,  $g(E)$  exhibits van Hove singularities, at which points it is impossible to differentiate  $H(E)$ , which for our application contains  $g(E)$ . Thus a Taylor series expansion is of questionable validity. Although the Fermi energy falls in a trough of the density of states curves, the effect of the high temperature Fermi function is to sample portions of adjacent peaks of  $g(E)$ . This is depicted in Fig. 3 for each structure at  $R_{WS} = 2.3 \text{ bohr}$ . Indeed, within an energy width of  $kT$  about the Fermi energy,  $g(E)$  may vary by more than a factor of two, especially for  $\epsilon$ -iron. It is for these reasons that we feel that a direct numerical integration of Eq. (3) is warranted.

For the numerical calculation it is necessary to determine  $\mu(T)$ , since it is contained within the expression for the Fermi function  $f(E)$ . This is accomplished by using the constraint that iron has electrons in its 4s, 3d valence band; hence  $n_e = 8$ . For practical calculations, the upper limits of the integrals in Eqs. (2) and (4) may be accurately truncated to about  $\mu(T) + 10 kT$ .

The integrations themselves were performed using the trapezoidal rule, due to the presence of  $g(E)$  in both integrands. Higher order integration techniques, as for example those employing cubic splines, were tried but deemed unnecessary and even misleading because of the complex structure in  $g(E)$ , and specifically the non-differentiable van Hove singularities. However, as noted above, when the density of energy grid points was more than doubled, the calculated specific heat changed by only  $\approx 1\%$ , and so our procedure should be more than adequate. Differentiations were carried out using a standard three-point formula (Burden, Faires, and Reynolds, 1978). All calculations were done with double precision declarations in the computer code.

#### 4. Calculational Results

The  $c_v$  curves calculated for our seven compressions are given in Fig. 4 ( $\gamma$ -iron) and in Fig. 5 ( $\epsilon$ -iron). The slight upward bend above approximately 2000 K clearly suggests the appearance of  $T^3$  behavior already above this temperature. This indicates that if the Sommerfeld expansion approximation is used, then another term should be included beyond that given by Eq. (10).

All the  $c_v$  curves in Figs. 4 and 5 show a tendency to level off at the highest temperatures shown, which can be easily understood from the  $g(E)$  plots in Figs. 1 and 2. The usual free-electron argument for  $c_v(T) \propto T$  is that  $\frac{kT}{E_F}$  electrons are excited, each receiving approximately  $kT$  in thermal energy. As can be seen in Figs. 1 and 2, however, the Fermi levels for both phases of iron lie in troughs between sharp peaks in  $g(E)$ . At sufficiently high temperature, the electronic distribution  $g(E)$  spans the two peaks. There is a tendency for new electronic excitations to be largely from the lower occupied peak to the higher empty peak; thus there is a constant excitation energy in contrast to one proportional to  $T$  as in the case of free electrons. This leads to a region of  $u_e(T) \propto T$ , and the tendency of the  $c_v$  curves in Figs. 4 and 5 to level off for awhile at high temperatures. Since features in  $g(E)$  scale roughly as  $(V/V_0)^{2/3}$ , it requires higher

temperatures to achieve this effect at the higher compressions, and so the behavior is most pronounced for the smallest compressions shown in the figures.

In order to convert  $R_{WS}$  values to geophysically sensible quantities, we need a pressure calibration. Typically pressure is calculated using the virial theorem. McMahan *et al.* (1981) discuss relative applicability of this method of pressure calculation. Local density calculations in general give poor pressures for the magnetic elements iron, cobalt, and nickel. Methods such as LMTO usually give the zero pressure volume for any particular element to within 6% of the correct value. For iron, cobalt, and nickel it is essential to use spin polarization for calculations in the ferromagnetic region. Yet at high pressures where the non-spin-polarized calculations should work well for the paramagnetic  $\epsilon$ -iron phase, the calculated pressures are still poor, possibly due to residual magnetic effects at high compression. For this reason we chose to use the best available  $p(V)$  curve, which is given by the semiempirical equation of state of Young and Grover (1984). Their 0 K isotherm was used to provide an approximate pressure scale for our band structure values of compression. Table 1 gives the pressure correspondence to  $R_{WS}$  values.

One purpose of this report is to provide a simple representation of the electronic specific heat of iron up to the largest temperatures possible for the purpose of making convenient geophysical estimates and in order to calculate shock Hugoniot for iron. We find that a standard linear  $c_v$  vs.  $T$  relation fits the lower temperature calculations while a derivative of a hyperbola fits the higher temperature values in a manner simple-to-parameterize, and hence useful for applications.

All of the specific heat curves begin to level off at approximately the same value of the specific heat. We model this essentially linear portion by running a least-squares fit to the specific heat curves truncated at the arbitrarily chosen ordinate cut-off of  $1.4 R$ . The resultant values of  $\beta$ , the coefficient of the linear aspect of the electronic specific heat, are given in Table 2 for  $\epsilon$ -iron and in Table 3 for  $\gamma$ -iron. A comparison is there

made between our calculated  $\beta$  values and  $\beta_{\text{Sommer}}$  as given by the standard expression derived from the Sommerfeld expansion, Eq. (10), divided by temperature. It is seen that our values for  $\gamma\text{-Fe}$  are slightly higher than those of Bukowski (1977) and do not decrease as rapidly with increasing compression as does  $\beta$  calculated from Eq. (10).

The internal energy curves, two examples of which are given in Fig. 6, can be closely fit by hyperbolae. For this reason the high temperature specific heat is here modeled as the analytic derivative of a hyperbolic internal energy:

$$c_v = c_0 + bT [1 + (T/\Theta_e)^2]^{-1/2}. \quad (11)$$

This parameterization may be more physically "meaningful" than a physics-blind polynomial fit. The parameter  $b$  behaves like a linear coefficient of electronic specific heat,  $\beta$ , while  $\Theta_e$  serves as a characteristic temperature in a way not too unsimilar to an Einstein  $\Theta_E$  for lattice specific heat.

Good fits with simple behavior of free parameters were obtained for the specific heat curves by restricting the range of fit to those temperatures and atomic volumes applicable to iron under conditions of geophysical interest. Tables 2 and 3 give the cutoff temperature,  $T_{\text{max}}$ , between the linear fit and the free-parameter fit. The parameters were varied to fit the compressions of  $R_{\text{WGS}} = 2.1, 2.2, 2.3$ , and  $2.4$  bohr for each structure separately. Those fits for  $2.2$  and  $2.3$  bohr are depicted in Fig. 7. The final parameters are given in Table 4.

From the density of states we also calculated the electronic free energy, the thermal electronic pressure, and the electronic Gruneisen parameter. Of course, these thermodynamic quantities arise from electronic contributions only, and are not total quantities.

The electronic free energy is given by

$$F_e(V, T) = u_e(V, T) - TS_e(V, T), \quad (12)$$

where the entropy

$$S_e(V, T) = \int_0^T \frac{c_v(V, T)}{T} dT. \quad (13)$$

Plots of  $F_e(T)$  for each iron phase at  $\rho=12.28 \text{ Mg m}^{-3}$  are shown in Fig. 6. Use of the Sommerfeld expansion leads to

$$F_e = u_{e,0} - \frac{\pi^2}{6} g(E_F) (kT)^2, \quad (14)$$

where  $u_{e,0}$  is the electronic internal energy at  $T=0 \text{ K}$ . At high temperature the free energy, like the internal energy, deviates from the parabolic approximate form and becomes somewhat linear such that the curve is approximately a hyperbola. This is caused, as discussed above, by the smearing effect of the Fermi function on the two large peaks due to d-bands near  $E_F$  in the  $g(E)$  function.

The thermal electronic contribution to the free energy is given by

$$\Delta F_e(V, T) = F_e(V, T) - F_e(V, T=0). \quad (15)$$

Thermal pressure due to excited conduction electrons is

$$\Delta p_e(V, T) = - \left( \frac{\partial \Delta F_e(V, T)}{\partial V} \right)_T. \quad (16)$$

Since we have band structure calculations for seven compressions we used cubic spline interpolation to generate a smooth curve for  $\Delta F_e$ , which was subsequently numerically differentiated. For the range of Earth core compression the electronic thermal pressure  $\Delta p_e \approx 6 - 12 \text{ GPa}$ .

An application of the thermal pressure results is the calculation of an electronic Gruneisen parameter. Thermodynamically, we may define the electronic Gruneisen parameter as

$$\bar{\gamma}_e = V \frac{\Delta p_e(V, T)}{\Delta u_e(V, T)} \quad (17)$$

(Zharkov and Kalinin, 1971). Following the approximations arising from use of the Sommerfeld expansion, Eq. (17) becomes

$$\gamma_e = \left( \frac{\partial \ln g(E_F)}{\partial \ln V} \right)_T. \quad (18)$$

The electronic Gruneisen parameter is more readily calculated from the following

expression equivalent to Eq. (18) (Bukowinski, 1977):

$$\beta = \beta_0 \left( \frac{V}{V_0} \right)^{\gamma_e} \quad (19)$$

Bukowinski's results for  $\gamma$ -iron are  $\beta_0 = 4.47 \pm 0.15 \text{ mJ K}^{-2} \text{ mol}^{-1}$  and  $\gamma_e = 1.5 \pm 0.1$ .

Log-log fits of our  $\beta$  values given in Tables 2 and 3 yield the following results:

For  $\gamma$ -iron:  $\beta_0 = 4.99 \pm 1.01 \text{ mJ K}^{-2} \text{ mol}^{-1}$  and  $\gamma_e = 1.27 \pm 0.03$ ;

for  $\epsilon$ -iron:  $\beta_0 = 5.06 \pm 1.01 \text{ mJ K}^{-2} \text{ mol}^{-1}$  and  $\gamma_e = 1.34 \pm 0.02$ .

The uncertainties are one standard deviation of the given quantity.

Direct numerical calculation of  $\gamma_e$  from Eq. (17) gave virtually identical results for the two phases of iron:  $1.32 \pm 0.21$  for  $\gamma$ -iron and  $1.32 \pm 0.43$  for  $\epsilon$ -iron. We found that the ratio  $\Delta p_e(V, T) / \Delta u_e(V, T)$  exhibited essentially no temperature dependence above 3000 K.

## 5. Applicability of results to the outer core

Our calculations are for pure iron in the hcp and fcc structures. The substance comprising the earth's outer core is neither pure iron nor in a solid phase. However, we argue on the basis of other recent research that the electronic thermodynamics of pure, crystalline, close-packed iron is similar to that of liquid iron and to that of iron alloyed with lighter, p-shell metals. In addition, the electronic properties of iron alloyed with another 3d-shell transition metal, such as nickel, appear to be predictable from the electronic structures of each metal in pure form. Thus electronic band structure calculations for close-packed iron can be cautiously applied to compositions and pressure and temperature conditions specified by current models of the outer core.

We assume that the liquid iron alloy of the outer core has close-packed coordination. This seems reasonable because of the high compressions of the core; for the pressure range between 100 and 200 GPa the volume difference between  $\gamma$  and liquid iron is 2% or less (Brown and McQueen, 1982), while the compression change is approximately

20%. Since the electronic thermodynamic parameters are essentially determined by the density of states, it appears that such parameters are not much affected by the particular form of close-packing represented by the iron atoms. Thus our results may apply to pure liquid iron under outer core conditions of pressure and temperature.

Recent studies indicate that at zero pressure, disordered iron possesses similar density of states to that of crystalline iron. Weir *et al.* (1983) used a tight-binding method to investigate the electronic states of amorphous or liquid iron. The density of states due solely to d-bands, and that due to s-bands, differed little between the disordered and crystalline cases. They speculate that the general mixing between s- and d-bands in non-symmetry directions in the crystal is sufficient to cause this similarity in the density of states.

In another theoretical study, Yokoyama *et al.* (1983) used a semi-empirical entropy scaling argument to calculate the electronic specific heat of liquid iron. Our calculation of  $c_v$ , extrapolated for  $\gamma$ -iron at  $T=1833$  K and  $\rho=7.01$   $Mg\ m^{-3}$  agrees almost exactly with their calculation for liquid iron at that temperature and density. At core pressures liquid iron would be more tightly packed; thus for the outer core the validity of these theories would be enhanced for high compression.

The electronic physics of alloys presents additional challenges to core modelers. A combination of light elements, particularly sulfur, oxygen, or hydrogen, is thought to form a liquid alloy with iron in the outer core (see, e.g., Ringwood, 1979). The proportion of light element, or elements, to iron is probably close to 20 mol %, according to shock wave and equation-of-state data.

Available band structure calculational results do not yet come close to covering all of the iron alloy compositions of interest to modelers of the core. However, enough work has been done to allow some tentative conclusions to be drawn about the applicability to the outer core of our pure crystalline iron calculation.

Using the APW method for nonmagnetic  $Fe_3Si$  Swintendick (1976) found that the density of states at  $E_F$  is predominantly associated with contributions from the iron sites. Koenig and Khan (1983) used the LMTO method to calculate the band structure of FeAl in the CsCl structure. They also found that at the Fermi level the density of states, and thus the electronic physical properties, are mainly controlled by the d-orbital electrons of iron. This conclusion is supported by the experimental work of Muir *et al.* (1982). Their measurements of the electrical resistivity of a series of  $Fe_3Si_{1-x}Al_x$  alloys (with  $0 \leq x \leq 1$ ) strongly suggest that the conductivity is dominated by electrons from the iron atoms.

Nickel is thought to be also alloyed with iron in the outer core. The electronic specific heat of such an alloy should be predictable because there exists a systematic trend in the density of states at the Fermi energy for the fcc 3d transition metals. Moruzzi *et al.* (1978) plot the density of states for 32 metals, including (in the fcc phase) cobalt, nickel, copper, and zinc. The Fermi energy systematically moves across density of states plots of nearly identical form as successive 3d elements are considered and 3d electrons added. For nickel the Fermi energy falls on a sharp peak, giving rise to a greater electronic specific heat than has iron.

The electronic specific heat for a dilute iron-nickel alloy can be predicted by considering how the density of states at the Fermi energy changes from the value of pure iron. This change is due to the altered number of average conduction electrons per atom of the alloy relative to the monatomic substance. According to the model of Morgan and Anders (1980), the core should have approximately 5.8 wt % nickel and 88.8 wt % iron. An iron-nickel alloy of this proportion would then have 5.9 mol % nickel. Since nickel has 10 conduction electrons and iron has 8, the alloy has an average of 8.1 conduction electrons per atom. We then assume that the total density of states of this alloy is nearly identical to that of pure iron, which is reasonable because the dilute element, nickel, displays density of states virtually indistinguishable from that of fcc iron

(Moruzzi *et al.*, 1978). The new Fermi energy demanded by 8.1 conduction electrons per atom yields a density of states at the Fermi level that is for core compressions 8 % less than the value for pure  $\gamma$ -iron. We then estimate, using the linear relationship given by Eq. (10), that the same ratio holds for the electronic specific heats. However, a similar analysis for 20 mol % sulfur or oxygen alloyed with iron gives an alloy electronic specific heat that is 15-20 % greater than that for pure  $\gamma$ -iron. Thus it appears that for the outer core the electronic effects due to nickel somewhat offset those due to sulfur or oxygen.

A numerical value for the electronic specific heat of the core can be obtained from Figs. 4 and 5. We used  $3600 \pm 500$  K as the temperature at the core-mantle boundary (CMB) and  $5100 \pm 500$  K for the center of the Earth. These temperature choices are justified by shock wave work on the equation of state of iron (Brown and McQueen, 1982; Shankland and Brown, 1985). We mapped this temperature region onto the  $c_v$  curves for our seven compressions and used PREM densities to further delineate the region of the plots applicable to the core. The  $c_v$  curve for  $R_{WS} = 2.4$  bohr corresponds for pure iron to a density of  $10.80 \text{ Mg m}^{-3}$ , which is close to the density in the core at a spherical shell containing half of the volume of the core. Choosing a temperature of  $T = 4200 \text{ K}$  as representative of this "average" core region, we find that pure iron under these "average" core conditions has an electronic specific heat  $c_v \approx 1.65 R$  for  $\gamma$ -iron and approximately  $1.70 R$  for  $\epsilon$ -iron.

Alloying with nickel and with sulfur or oxygen probably, as discussed above, raises the electronic specific heat approximately 10 % relative to that of  $\gamma$ -iron. However, because the density of states is relatively constant for energies near the Fermi energy for  $\epsilon$ -iron, a dilute  $\epsilon$ -iron alloy probably has an electronic specific heat the same as the value for pure  $\epsilon$ -iron. Since the close-packed liquid alloy of the outer core is not clearly more similar in form to one or the other of the fcc and hcp structures, we conclude that the effect of alloying is to slightly raise the electronic specific heat relative to a value of

$1.7 R$  for pure iron under "average" core conditions. Therefore, we believe that  $c_v = 1.8 \pm 0.5 R$  characterizes the electronic specific heat of the core. The uncertainty in this value depends on several factors: numerical errors, the approximations necessary for the band structure calculation, and the range of values ascribable to core densities. Since alteration of the Brillouin zone sampling density and the inclusion of relativistic effects each changed the resultant electronic specific heat by only 1 %, and since variation of differentiation and integration techniques also had negligible effect, the quoted uncertainty reflects the values assigned to the range of conditions in the core.

The heat capacity of the core can be easily estimated from the total specific heat,  $c_v$ , and from the mean atomic weight,  $\bar{m}$ . Use of  $\bar{m} = 49.3 \text{ g/mol}$  (Watt *et al.*, 1975) and  $c_v = 3R + c_v = 4.8R$  leads to a total core heat capacity of  $C = 1.6 \times 10^{27} \text{ J K}^{-1}$ . This is one-quarter of the heat capacity of the entire Earth.

The electronic specific heat and Gruneisen parameter are also useful in calculation of the temperature at the core-mantle boundary. However, use of our values of  $c_v$  and  $\gamma_e$  do not significantly alter the results given by Brown and McQueen (1985).

## 6. Conclusions

Application of the LMTO method of electronic band structure calculation for  $\epsilon$ -iron and  $\gamma$ -iron has yielded density of electronic states for each phase under seven compressions more than spanning the compressions of the Earth's core. These densities of states curves are of complex form because of contributions from d-shell electrons. However, the two close-packed structures yield similar density of states. Electronic thermodynamic quantities, such as the electronic specific heat and the electronic Gruneisen parameter, are determined by the complex form of the density of states curves near the Fermi level. This complicated form causes the electronic specific heat to deviate at core temperatures from the standard metal linear relationship:  $c_v = \beta T$ . A simple parameterization of the high temperature portion of the electronic specific heat curves has been provided.

A characteristic core value of the electronic specific heat has been determined to be  $1.8 R$ . This value reflects consideration of the fact that the outer core is not pure, crystalline iron. Recent research indicates that the electronic density of states of liquid iron is similar to that of pure, solid iron. Moreover, the density of states of iron alloyed with nickel or a lighter, p-shell metal seems to differ from that of pure iron in a predictable, minor way. Under high compression this similarity in the density of states should be enhanced due to the regularity of atomic close-packing. Thus the material comprising the outer core may be investigated in electronic thermodynamic properties by the results of iron band structure calculations.

The heat capacity of the core is calculated to be one-quarter that of the entire Earth. An electronic Gruneisen parameter of  $1.3 \pm 0.4$  is also determined for iron under core conditions. This value does not lead to a significant reevaluation of the core-mantle boundary temperature ascribed by Brown and McQueen (1985).

This study provides new constraints on Earth core electronic thermodynamical parameters. Models of the core can benefit from these new constraints. Further constraints will be provided by alloy band structure calculations and experimental high pressure research.

### **Acknowledgments**

This work was supported by the National Science Foundation under grant EAR-8501390. We thank D. Young for the pressure calibration for  $\epsilon$ -iron and R. Merrill and Y. Sato-Sorensen for helpful discussions. Part of this work was performed under the auspices of the U. S. Department of Energy by Lawrence Livermore National Laboratory under Contract No. W-7405-Eng-48.

## REFERENCES

- Andersen, O. K., 1975. Linear methods in band theory. *Phys. Rev. B*, 12: 3060-3083.
- Andersen, O. K., 1983. In: P. Phariseau (Editor), *The Electronic Structure of Complex Systems*. Plenum, New York, NY.
- Andersen, O. K. and Jepsen, O., 1977. Advances in the theory of one-electron energy states. *Physica*, 91B: 317-328.
- Ashcroft, N. W. and Mermin, N. D., 1976. *Solid State Physics*. Saunders College, Philadelphia, PA.
- Brown, J. M. and McQueen, R. G., 1982. The equation of state for iron and the Earth's core. In: Akimoto, S. and M. H. Manghnani (Editors), *Advances in Earth and Planetary Sciences*. Vol. 12, *High-Pressure Research in Geophysics*. Riedel, Boston, pp. 611-623.
- Brown, J. M. and McQueen, R. G., 1985. Phase transitions, Gruneisen parameter and elasticity for shocked iron between 100 GPa and 400 GPa; submitted for publication.
- Brown, P., Capellmann, H., Deportes, J., Givord, D. and Ziebeck, K., 1983. *J. Magn. and Magn. Matl.*, 31-34: 295.
- Bukowinski, M. S. T., 1976. On the electronic structure of iron at core pressures. *Phys. Earth Planet. Inter.*, 13: 57-66.
- Bukowinski, M. S. T., 1977. A theoretical equation of state for the inner core. *Phys. Earth Planet. Inter.*, 14: 333-344.
- Burden, R., Faines, J., and Reynolds, A., 1978. *Numerical Analysis*, 2nd Ed. Prindle, Weber, and Schmidt; Boston, MA.
- Callaway, J. and C. S. Wang, 1977. *Phys. Rev. B*, 16: 2095.
- Choy, G. L. and Cormier, V. F., 1983. The structure of the inner core inferred from short-period and broadband GDSN data. *Geophys. J. R. Astr. Soc.*, 72: 1-21.
- Cort, G., Taylor, R. D. and Willis, J. O., 1982. *J. Appl. Phys.*, 53: 2064.
- Dziewonski, A. M. and Anderson, D. L., 1981. Preliminary reference Earth model. *Phys. Earth Planet. Inter.*, 25: 297-356.
- Jamieson, J. C. and Lawson, A. W., 1962. X-ray diffraction studies to 100 kbar. *J. Appl. Phys.*, 33: 776-780.
- Janak, J. F., 1974. Simplification of total-energy and pressure calculations in solids. *Phys. Rev. B*, 9: 3985-3988.
- Jepsen, O., O. K. Andersen and Mackintosh, A. R., 1975. Electronic structure of hcp transition metals. *Phys. Rev. B*, 12: 3084-3103.

- Johnson, W. B., Anderson, J. R. and Papaconstantopoulos, D. A., 1984. Fermi surface of iron under pressure. *Phys. Rev. B*, 29: 5337-5348.
- Koenig, C. and Khan, M. A., 1983. Self-consistent electronic structure of FeAl. *Phys. Rev. B*, 27: 6129-6135.
- McMahan, A. K. and Ross, M., 1977. High-temperature electron-band calculations. *Phys. Rev. B*, 15: 718-725.
- McMahan, A. K., Skriver, H. L. and Johansson, B., 1981. The s-d transition in compressed lanthanum. *Phys. Rev. B*, 23: 5016-5029.
- Masters, G. and F. Gilbert, 1981. Structure of the inner core inferred from observations of its spheroidal shear modes. *Geophys. Res. Lett.*, 8: 569-571.
- Morgan, J. W. and E. Anders, 1980. Chemical composition of Earth, Venus, and Mercury. *Proc. Nat. Acad. Sci. USA*, 77: 6973-6977.
- Moruzzi, V., Janak, J. and Williams, A., 1978. *Calculated Electronic Properties of Metals*. Pergamon, New York, NY.
- Muir, W. B., Budnick, J. I. and Raj, K., 1982. Electrical resistivity and the band structure of  $Fe_3Si_{1-x}Al_x$  alloys. *Phys. Rev. B*, 25: 726-729.
- Ringwood, A. E., 1979. *Origin of the Earth and Moon*. Springer-Verlag, New York, NY.
- Shankland, T. J. and Brown, J. M., 1985. Homogeneity and temperatures in the lower mantle. *Phys. Earth Planet. Inter.*, 38: 51-58.
- Skriver, H. L., 1984. *The LMTO Method*. Springer, Berlin.
- Slater, J. C., 1974. The self-consistent field for molecules and solids. In: *Quantum Theory of Molecules and Solids*, Vol. 4. McGraw-Hill, New York, NY.
- Swintendick, A. C., 1976. *Solid State Commun.*, 19: 511-515.
- Vinokurova, L. I., Gapotchenko, A. G., Jtskevich, E. S., Kulatov, E. T. and Kulikov, N. I., 1979. *Sov. Phys. - JETP*, 49: 834.
- von Barth, U. and Hedin, L., 1972. *J. Phys. C*, 5: 1629.
- Watt, J. P., Shankland, T. L. and Mao, N. H., 1975. Uniformity of mantle composition. *Geology*, 3: 91-94.
- Weir, G. F., Howson, M. A., Gallagher, B. L. and Morgan, G. J., 1983. Hybridization in amorphous metals. *Philos. Mag. B*, 47: 163-176.
- Williamson, D., Bukshpan, S. and Ingalls, R., 1972. *Phys. Rev. B*, 6: 4194.

Yokoyama, I., Ohkoshi, I., and Satoh, T., 1983. J. Phys. F: Met. Phys., 13: 729.

Young, D. A. and Grover, R., 1984. Theory of the iron equation of state and melting curve to very high pressures. In: J. R. Asay, R. A. Graham and G. K. Straub (Editors), Shock Waves in Condensed Matter - 1983. Elsevier, pp. 65-67.

Zharkov, V. and Kalinin, V., 1971. Equations of State for Solids at High Pressures and Temperatures. Consultants Bureau, New York, NY.



TABLE 1 Pressure calibration at $T = 0K$		
$R_{WS}(\text{bohr})$	$\rho(\text{Mg m}^{-3})$	$p(\text{GPa})$
2.6	8.50	3.9
2.5	9.56	35.8
2.4	10.81	90.6
2.3	12.28	182
2.2	14.03	333
2.1	16.14	580*
2.0	18.68	977

\* (pressure values beyond 500 GPa are extrapolated beyond the empirical model)

TABLE 2 Linear electronic specific heat parameters for $\epsilon$ -iron*					
$R_{ws}$ (bohr)	$V/V_0$	density ( $Mg\ m^{-3}$ )	$T_{max}$ ( $K$ )	$\beta$ ( $mJ\ K^{-2}mol^{-1}$ )	$\beta_{Somm}$ ( $mJ\ K^{-2}mol^{-1}$ )
2.6	0.966	8.50	2480	4.93	3.49
2.5	0.859	9.56	2940	4.09	2.93
2.4	0.760	10.81	3480	3.50	2.46
2.3	0.669	12.28	4140	2.95	2.06
2.2	0.585	14.03	4920	2.43	1.74
2.1	0.509	16.13	5880	2.05	1.47
2.0	0.440	18.68	7060	1.72	1.28

\* ( $\rho_0=8.28Mg\ m^{-3}$ )

TABLE 3 Linear electronic specific heat parameters for $\gamma$ -iron*					
$R_{ws}$ (bohr)	$V/V_0$	density ( $Mg\ m^{-3}$ )	$T_{max}$ ( $K$ )	$\beta$ ( $mJ\ K^{-2}mol^{-1}$ )	$\beta_{Somm}$ ( $mJ\ K^{-2}mol^{-1}$ )
2.6	0.923	8.50	2580	4.59	4.51
2.5	0.821	9.56	3020	3.89	3.78
2.4	0.726	10.81	3580	3.31	3.16
2.3	0.639	12.28	4280	2.77	2.64
2.2	0.559	14.03	5080	2.37	2.18
2.1	0.487	16.13	6020	1.98	1.84
2.0	0.420	18.68	7080	1.70	1.45

\* ( $\rho_0=7.94Mg\ m^{-3}$ )

TABLE 4 Electronic specific heat fit parameters for $\gamma$ -iron			
$R_{ws}(\text{bohr})$	$c_0(J\ K^{-1}\text{mol}^{-1})$	$\Theta_e(K)$	$b(mJ\ K^{-2}\text{mol}^{-1})$
2.4	-2.10	5500	4.73
2.3	-4.33	5900	4.73
2.2	-6.69	6300	4.73
2.1	-9.19	6700	4.73

Electronic specific heat fit parameters for $\epsilon$ -iron			
$R_{ws}(\text{bohr})$	$c_0(J\ K^{-1}\text{mol}^{-1})$	$\Theta_e(K)$	$b(mJ\ K^{-2}\text{mol}^{-1})$
2.4	-1.97	5700	4.73
2.3	-4.20	6100	4.73
2.2	-6.56	6550	4.73
2.1	-9.32	7000	4.73

## Figure captions

Fig. 1.  $\gamma$ -iron density of states for  $R_{WS} = 2.2, 2.3, 2.4$ , and  $2.5$  bohr. The vertical line in each plot indicates the Fermi energy.

Fig. 2.  $\epsilon$ -iron density of states for  $R_{WS} = 2.2, 2.3, 2.4$ , and  $2.5$  bohr. The vertical line in each plot indicates the Fermi energy.

Fig. 3. Density of states and Fermi function  $f(E)$  for  $\gamma$ -iron (top) and  $\epsilon$ -iron (bottom). The maximum ordinate value for  $f(E)$  is 1. The long-dashed curve is  $f(E)$  for  $T = 0$  K, the short-dashed curve is for  $T = 5000$  K, and the dot-dashed curve is for  $T = 10,000$  K.

Fig. 4. Electronic specific heat for  $\gamma$ -iron. Curves are shown for the 7 compressions given in Table 1. From top to bottom the curves successively correspond to increasing compression. The small-scale fluctuations indicate the finiteness of the energy difference between successive values of the density of states curves.

Fig. 5. Electronic specific heat for  $\epsilon$ -iron. Curves are shown for the 7 compressions given in Table 1. From top to bottom the curves successively correspond to increasing compression. The small-scale fluctuations indicate the finiteness of the energy difference between successive values of the density of states curves.

Fig. 6. Electronic energy for  $\gamma$ -iron (top) and  $\epsilon$ -iron (bottom). The solid curves represent the internal energy,  $u_e(T)$ , and the dashed curves represent the free energy,  $F(T)$ .

Fig. 7. Parameterized fit to the electronic specific heat of  $\gamma$ -iron (top) and  $\epsilon$ -iron (bottom). See Table 4 for the parameters used. The dotted line represents the linear fit of  $c_v$ , with  $T \leq T_{\max}$ . The fit is shifted in order to pass through the origin. The dashed curve is the parameterized fit to  $c_v$ , with  $T \geq T_{\max}$ .

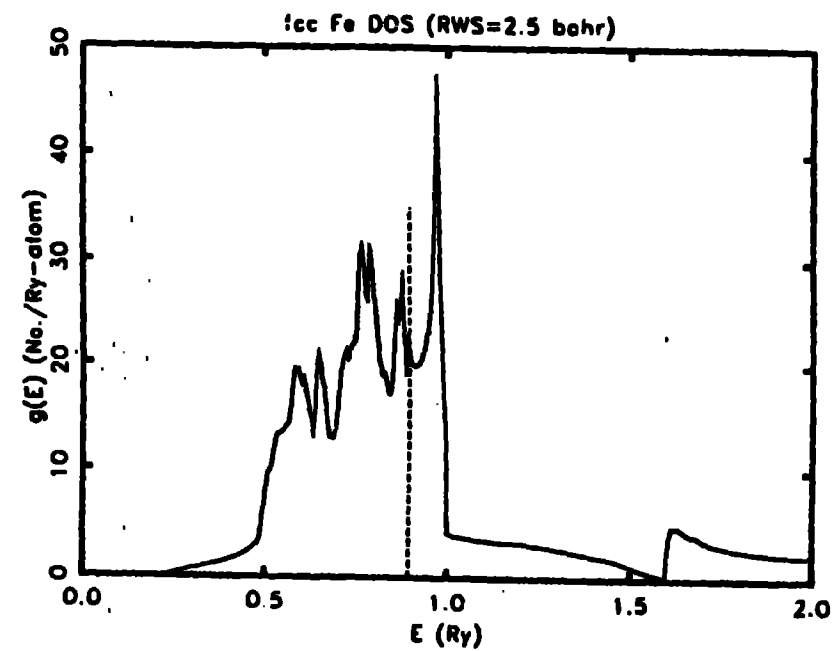
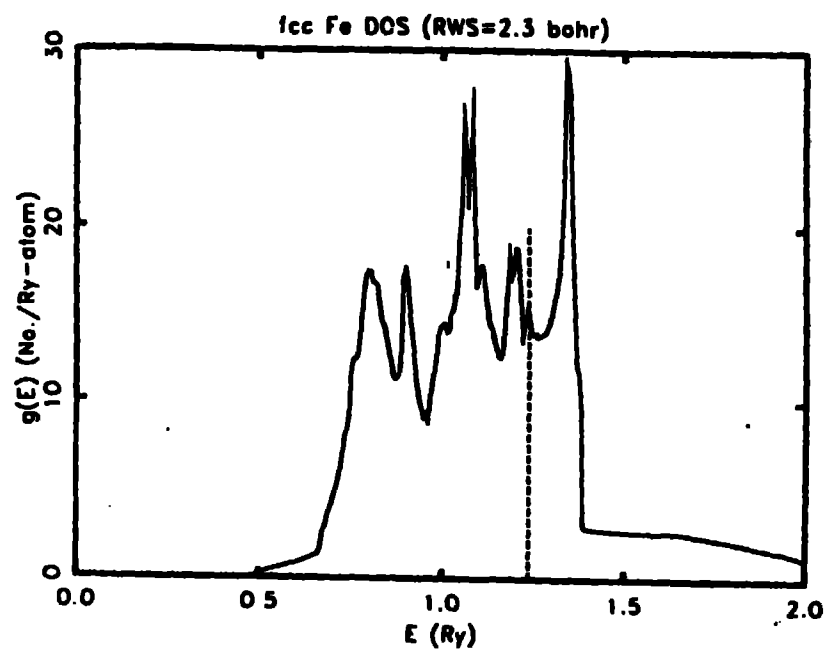
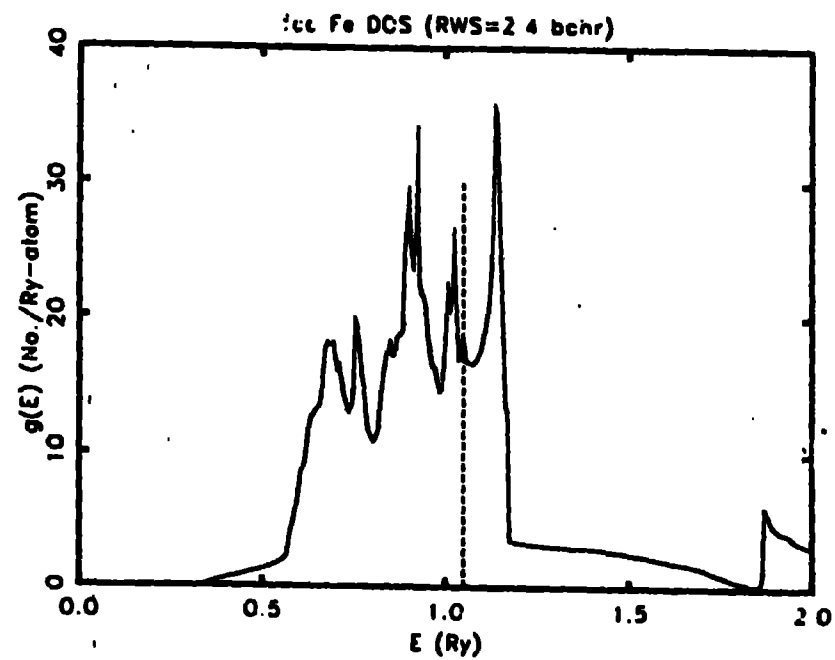
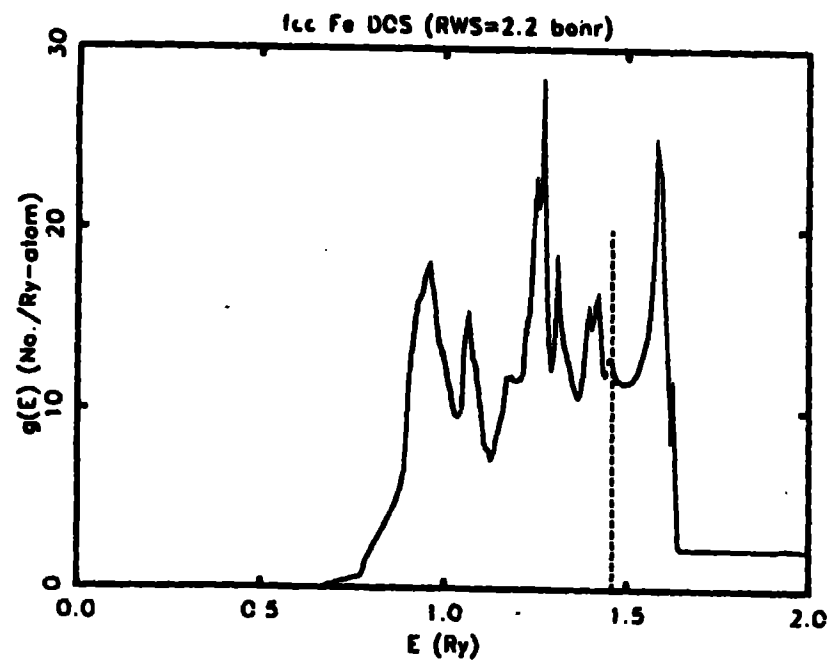


Fig. 1

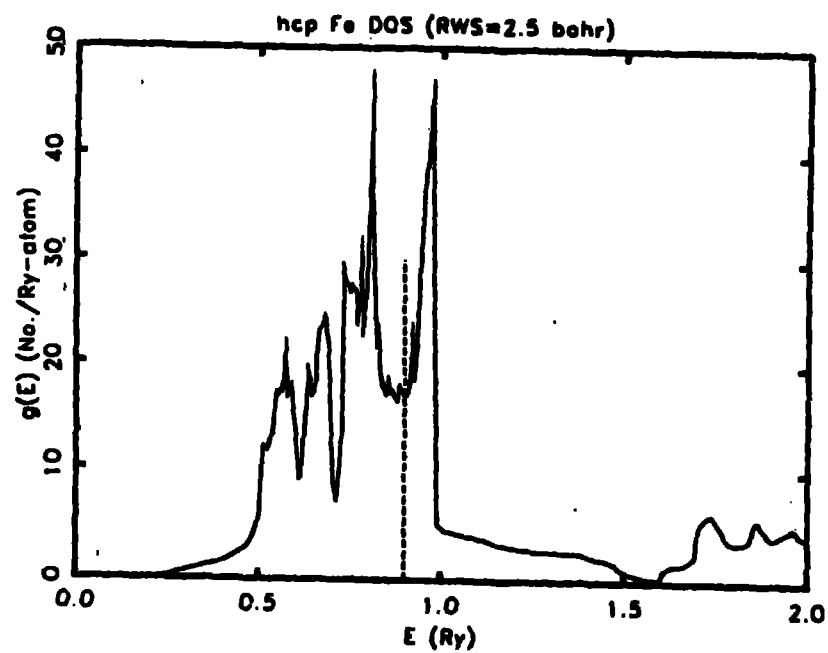
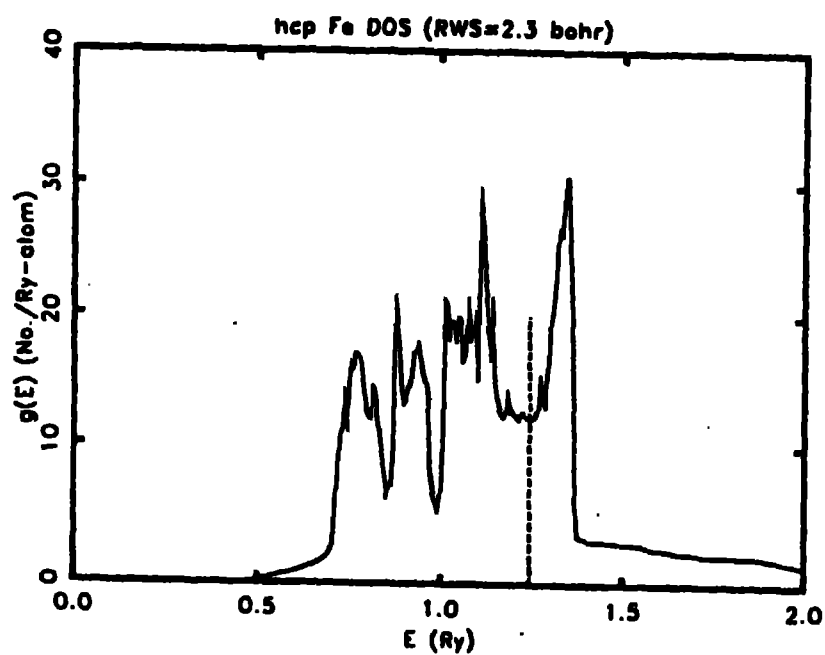
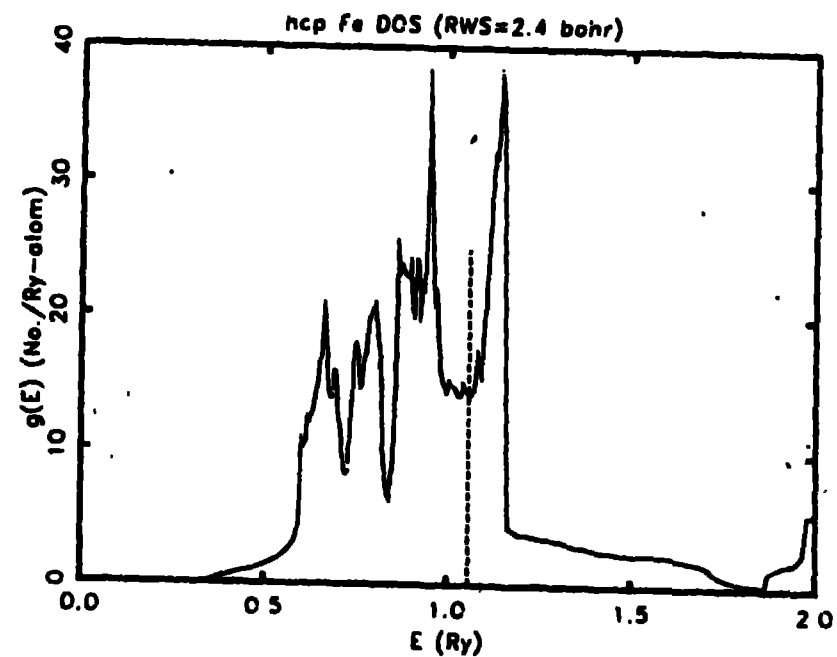
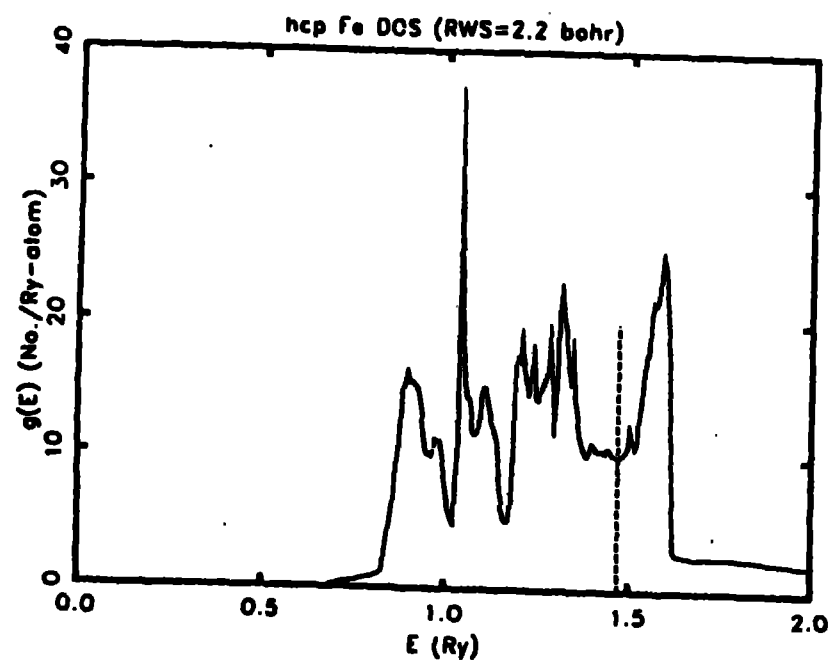
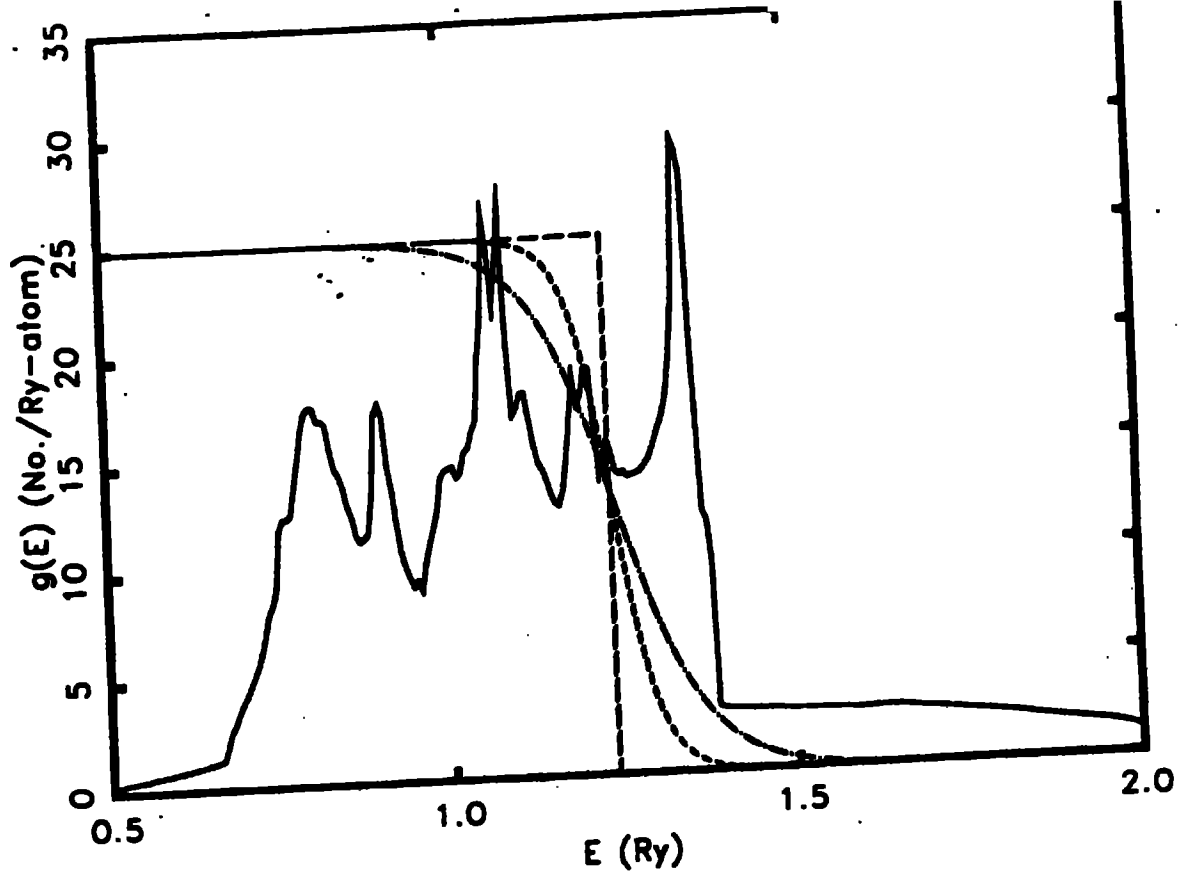


Fig. 2



hcp Fe DOS (RWS=2.3 bohr)

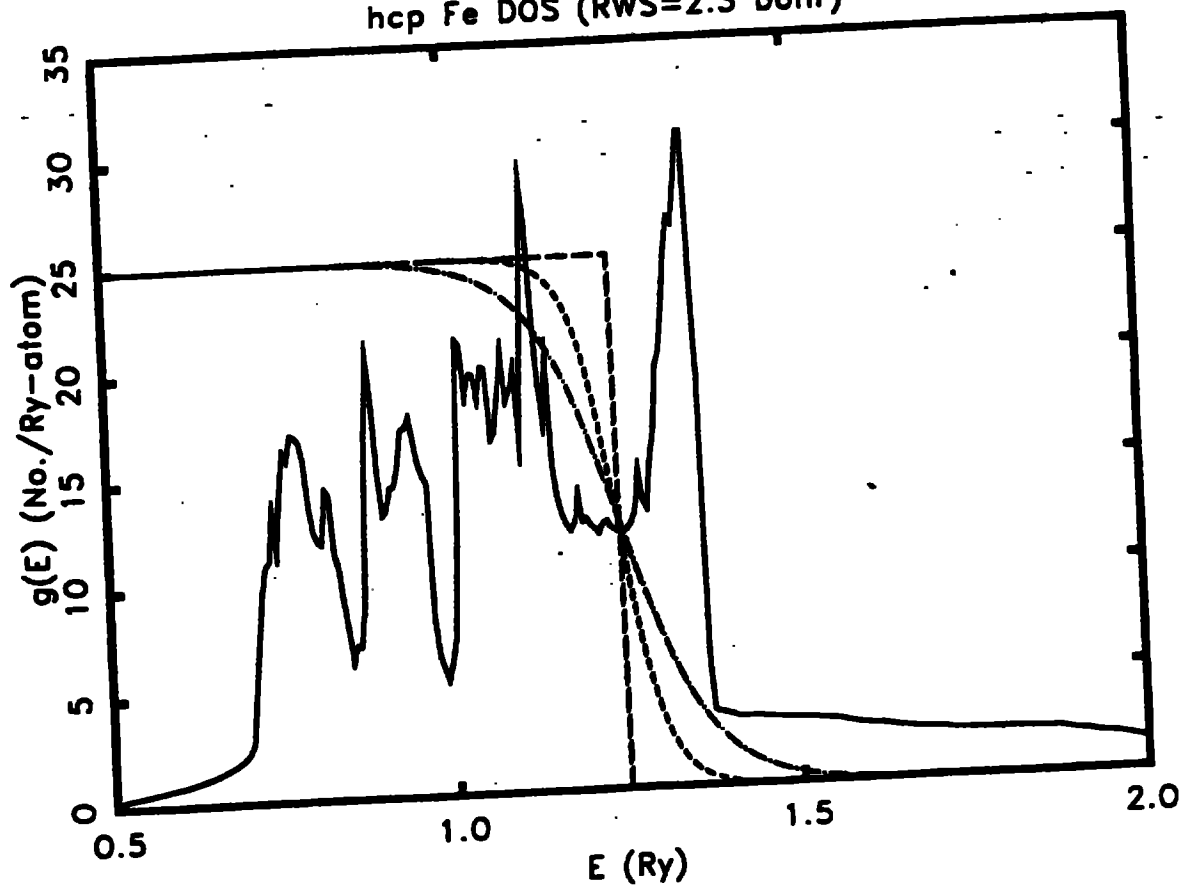


Fig. 3

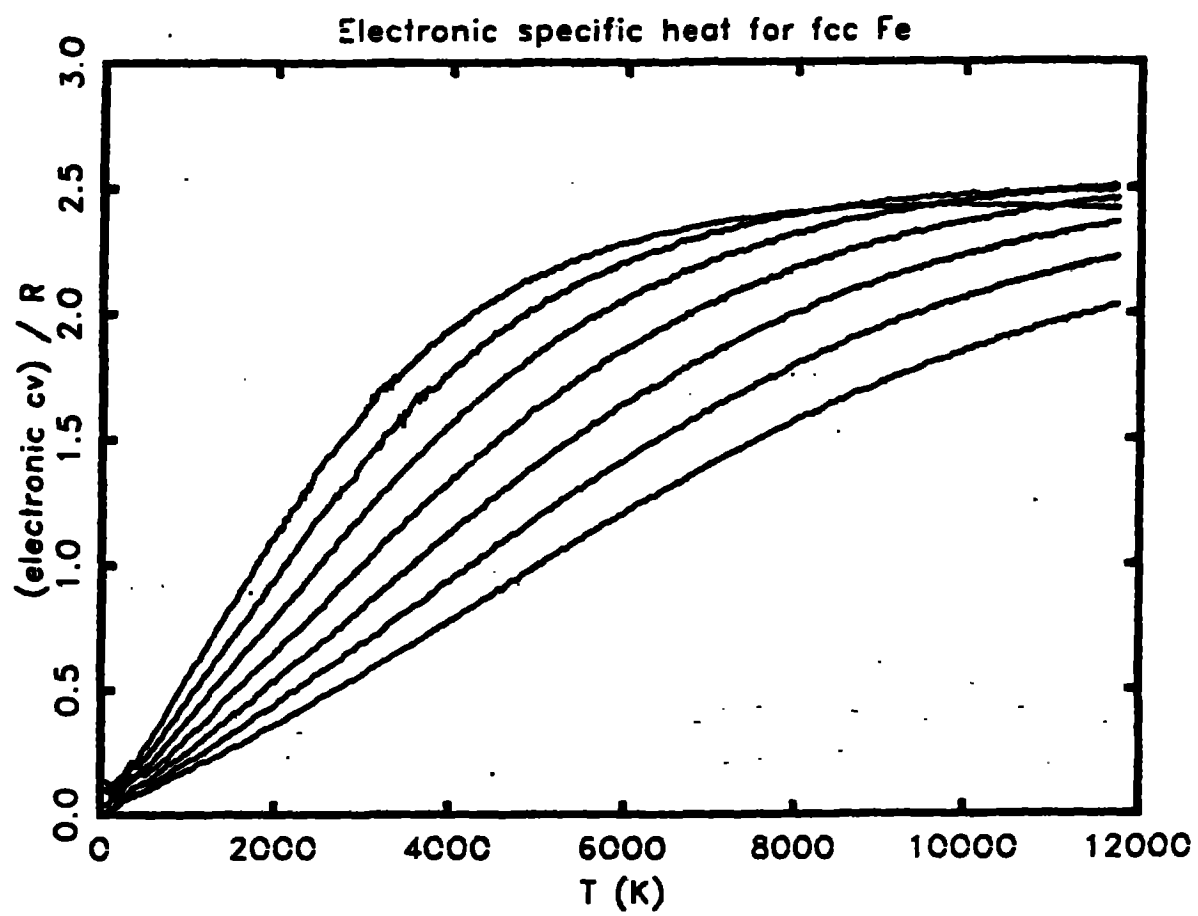


Fig. 4

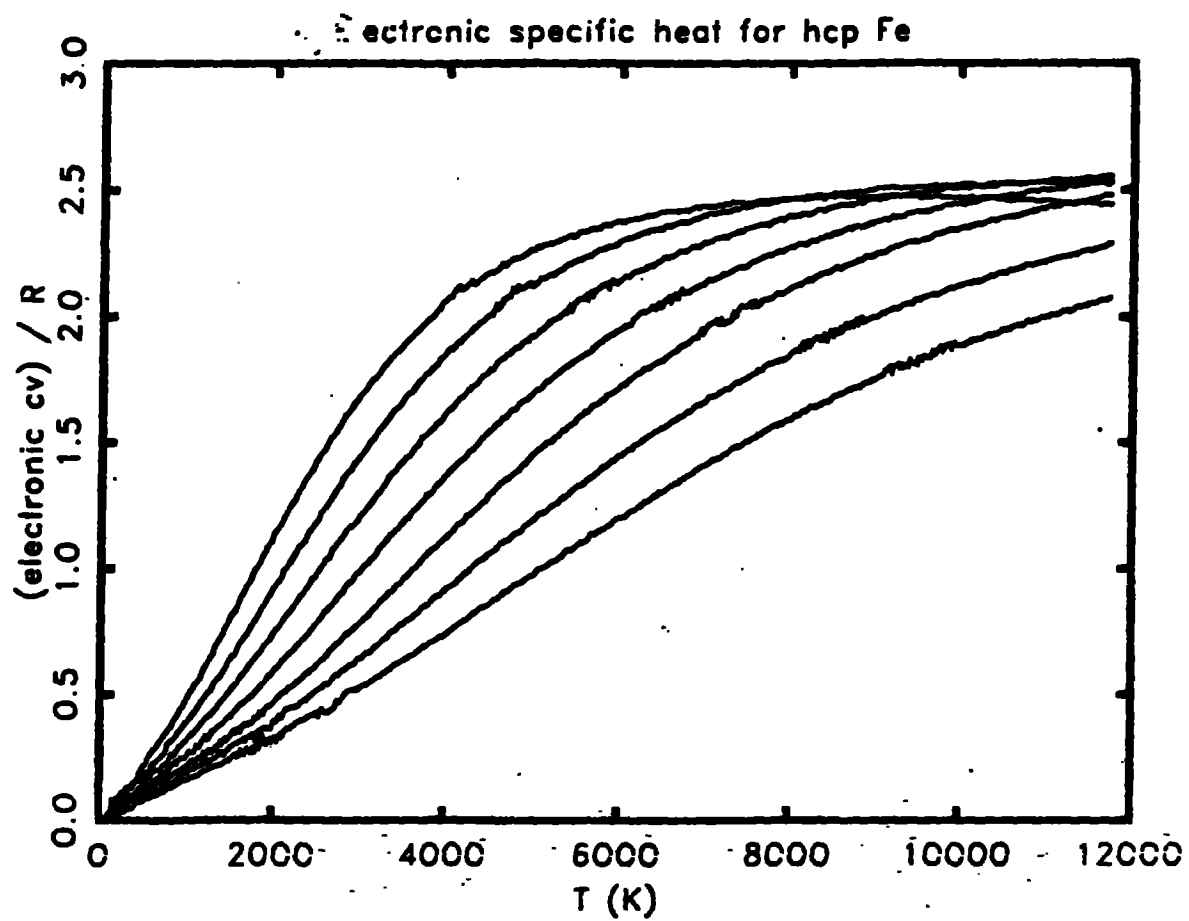


Fig. 5

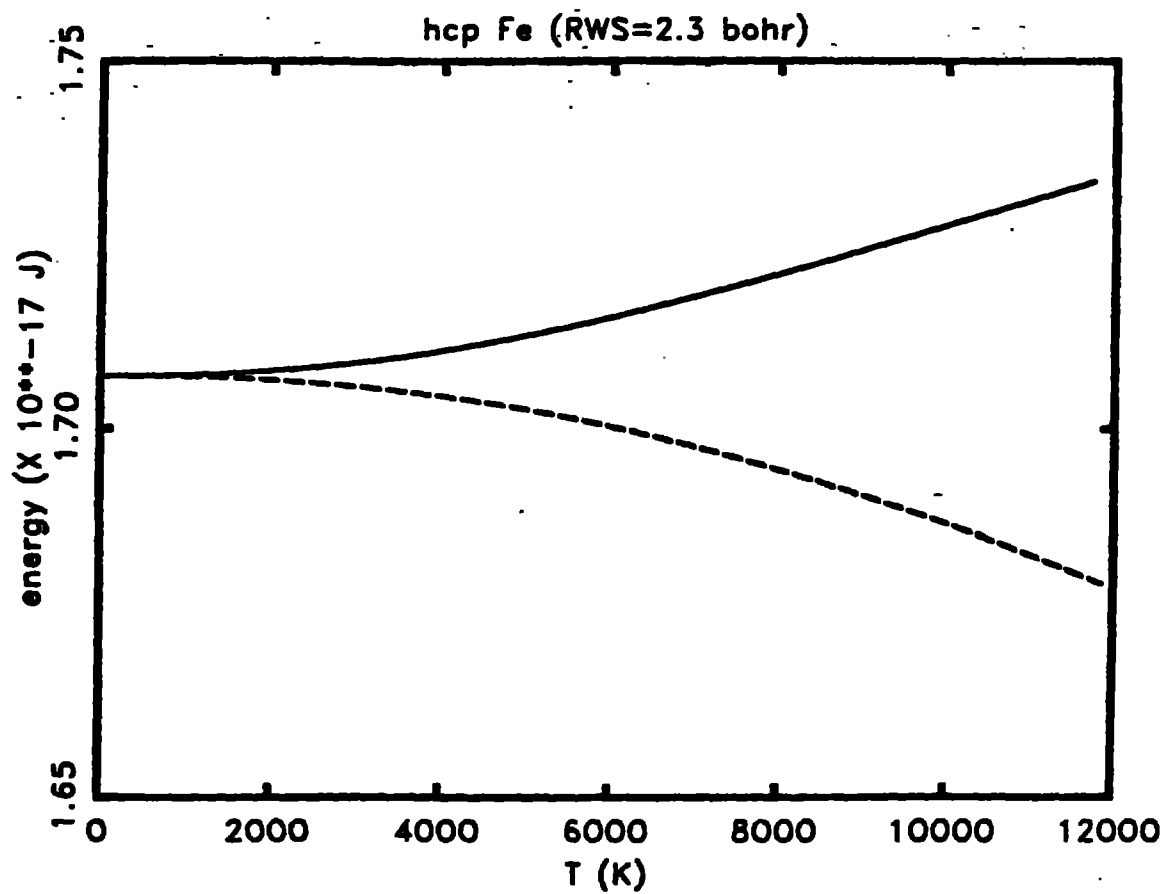
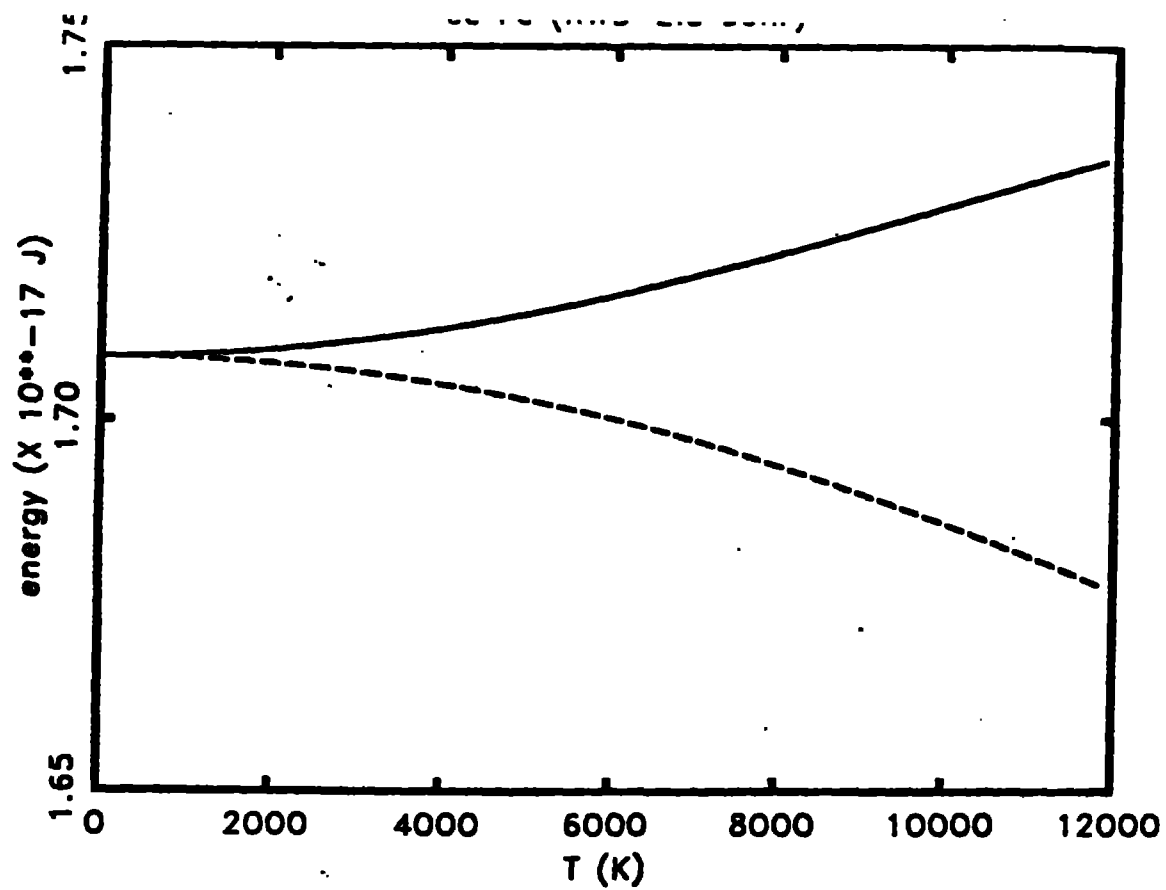


Fig. 6

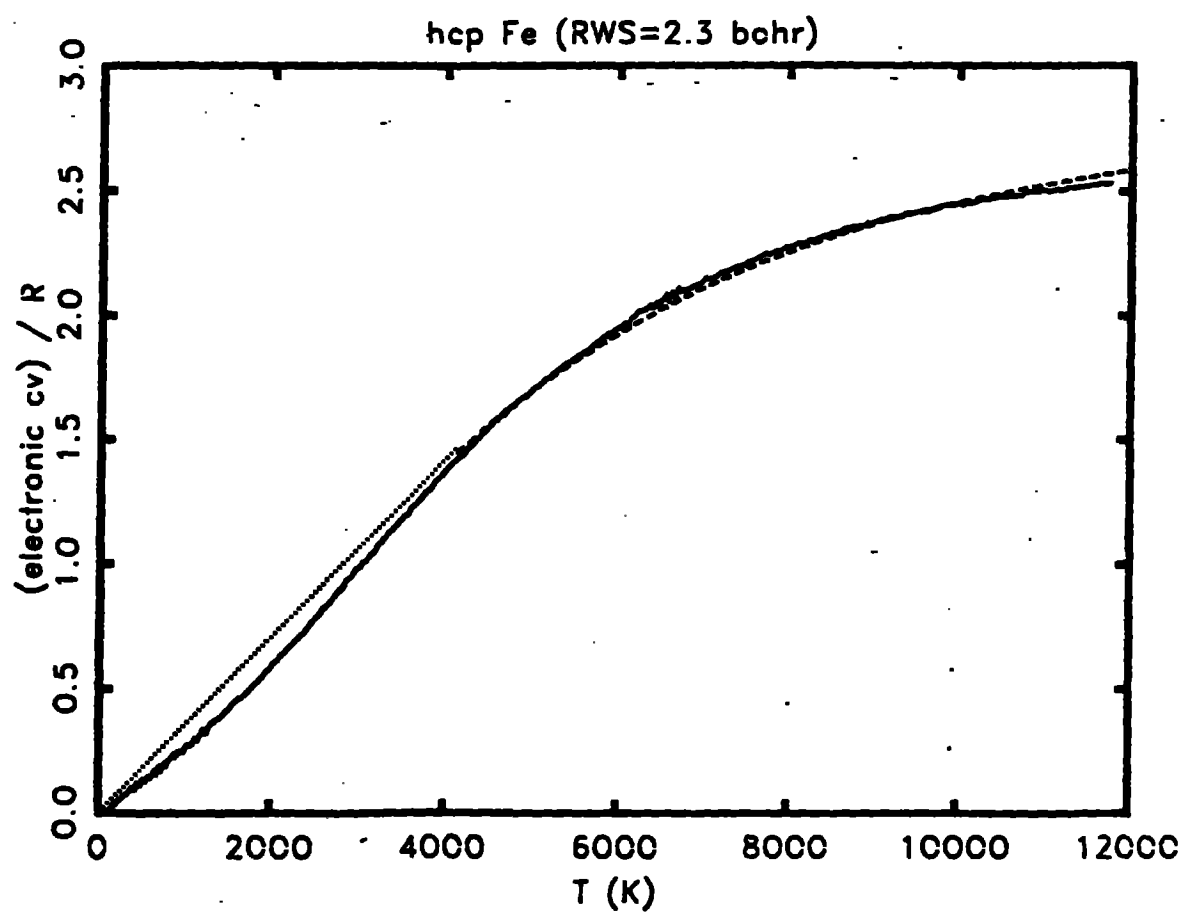
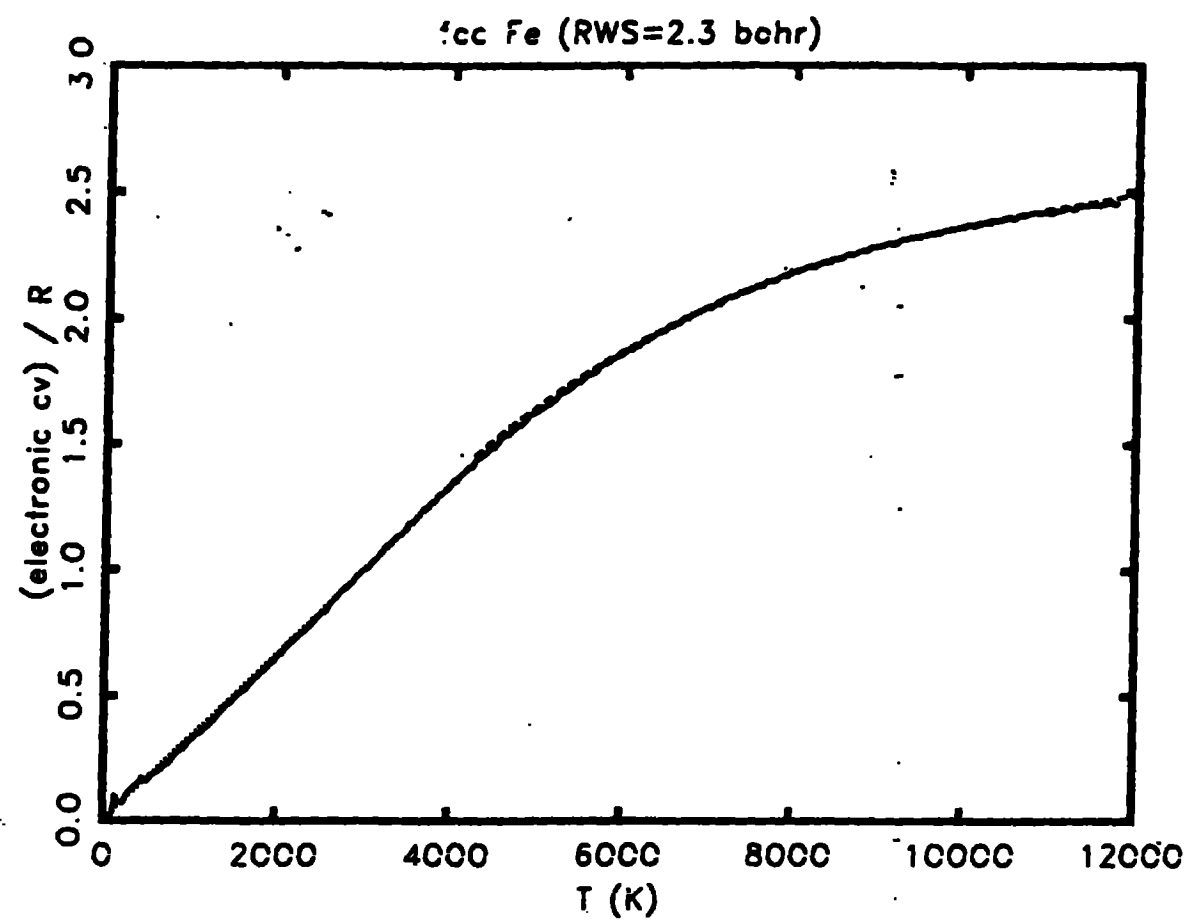


Fig. 7